Autothermal Oxidative Coupling of Methane: Steady-State Multiplicity over Mn-Na_2WO_4/SiO_2 at Mini-Plant Scale

Abigail Perez Ortiz[1,*], Alberto Penteado[1], Tim Karsten[1], Erik Esche[1], Vitor Grigull[2], Reinhard Schomäcker[3], and Jens-Uwe Repke[1]

DOI: 10.1002/cite.202100195

An experimental study of the potential autothermal reactor operation for the ethylene production via oxidative coupling of methane based on the ignition-extinction behavior for a Mn-Na_2WO_4/SiO_2 catalyst is presented. The possibility of benefiting from the heat released during the reaction is analyzed. The effect of different process variables, challenges, and limitations on the autothermal oxidative coupling of methane reactor operation are investigated in which a moderately large amount of heat appears.

Keywords: Autothermal operation, Ignition-extinction behavior, Oxidative coupling of methane, Reaction engineering

Received: November 03, 2021; *accepted:* March 07, 2022

1 Introduction

The oxidative coupling of methane (OCM) is an attractive concept for ethylene production due to its industrial potential for using different methane-rich feedstocks such as natural gas and biogas [1]. The main challenges for OCM implementation at commercial scale are related to the high reaction temperatures and low product yield (C_2) as a result of the deep oxidation of methane (CH_4) and C_{2+} products in the gas phase.

The OCM reaction network is quite complex since it involves not only different reactions on the catalytic surface, but also comprises reactions in the gas phase [2]. Many macro- and microkinetic models have been developed for OCM, where one of the most well-known was established by Stansch et al. [3]. Tab. 1 illustrates the exothermic nature of the most relevant OCM reactions. The C_2 coupling reactions are exothermic, but the exothermicity of the undesired side reactions is even higher. The desired C_2 hydrocarbon products, as well CH_4 can undergo total oxidation and hot-spots are prompt to appear on the catalyst surface.

Potential solutions to the control of the heat released during the reaction are the development of a low-temperature active and selective catalyst, and the control of harsh partial oxidation reaction conditions. In this regard, the temperature control is critical for OCM. Poor temperature control will lead to hot-spot formation and a decrease in catalyst activity due to a temperature rise in the catalyst bed of about 150 K, which results in a loss of surface area. [4].

Most of the lab-scale packed bed reactors are operated in a pseudo-isothermal regime [5]. However, for larger scales an adiabatic or near adiabatic operation seems to be the most feasible option [6], where the reaction temperature control is coupled with heat exchange between the inlet, reaction, and outlet gas resulting in an "autothermal" operation. An autothermal reaction control is used with packed bed reactors if the energy released by moderately exothermic reactions is utilized to heat the reactor feed to the ignition temperature of the catalyst [7].

Such a mode of operation would save energy that should be supplied to perform the process, and this will lower capital and operational expenses. Thus, it is important to identify the conditions for the autothermal operation and parameters that allow such a regime.

Since the optimum operation point of autothermal reactors falls on the ignited branch close to the extinction point, the determination of the location of the extinction point, which defines the boundary of the region of autothermal operation, is an important first step [8].

For these objectives, an understanding of the ignition-extinction behavior as well as hysteresis is relevant to

[1]Abigail Perez Ortiz, Dr.-Ing. Alberto Penteado, Tim Karsten, Dr.-Ing. Erik Esche, Prof. Dr.-Ing. habil. Jens-Uwe Repke
a.perezortiz@tu-berlin.de
Technische Universität Berlin, Fachgebiet Dynamik und Betrieb technischer Anlagen, Sekr. KWT 9, Straße des 17. Juni 135, 10623 Berlin, Germany.

[2]Vitor Grigull
ECO Erneuerbare Energien GmbH, Tobagostraße 5, 27356 Rotenburg (Wümme), Germany.

[3]Prof. Dr. Reinhard Schomäcker
Technische Universität Berlin, Institut für Chemie, Sekr. TC 8, Straße des 17. Juni 124, 10623 Berlin, Germany.

Table 1. Standard enthalpy of reaction values for selected OCM exothermic reactions.

Reaction	$-\Delta H^0_{Rx}$ [kJ mol_{CH4}]
$CH_4 + 0.5\,O_2 \rightarrow 0.5\,C_2H_4 + H_2O$	141
$CH_4 + 0.25\,O_2 \rightarrow 0.5\,C_2H_6 + 0.5\,H_2O$	88
$CH_4 + 1.5\,O_2 \rightarrow CO + 2\,H_2O$	519
$CH_4 + 2\,O_2 \rightarrow CO_2 + 2\,H_2O$	802

develop an autothermal concept. The autothermal procedure assumes the existence of several operating states (hysteresis). Different outlet conversions can be obtained at the same conditions, depending on the transient change of certain variables during the reactor operation.

In the present study, different operation parameters are analyzed to identify the ignition-extinction catalyst behavior and potential autothermal operation mode of the reactor.

2 Materials and Methods/Experiments

2.1 Catalyst Preparation

One of the best-known catalysts is Mn-Na_2WO_4/SiO_2 due to its performance and long-term stability at high temperatures required for OCM [9–11].

For the catalyst preparation, manganese(II) nitrate tetrahydrate ($Mn(NO_3)_2{\cdot}4H_2O$, >97 %), sodium tungstate dihydrate ($Na_2WO_4{\cdot}2H_2O$, >99 %) were purchased from Honeywell and used as precursors. Amorphous SiO_2 with grain sizes ranging 35–60 mesh particle size (silica gel, Davisil Grade 636) was purchased from Sigma-Aldrich.

A catalyst containing 1.9 % Mn and 5 % Na_2WO_4, expressed as weight percentages on SiO_2, was prepared via incipient wetness impregnation (IWI) method [12, 13]. An aqueous solution with appropriate concentration of $Mn(NO_3)_2{\cdot}4H_2O$ was added to silica gel, then dried at 373 K overnight. Afterwards, a $Na_2WO_4{\cdot}2H_2O$ solution with the corresponding concentration was added dropwise to the solid. The catalyst was dried at 373 K overnight and calcined in air at 1173 K using a heating rate of 10 K min^{-1} for 1.5 h.

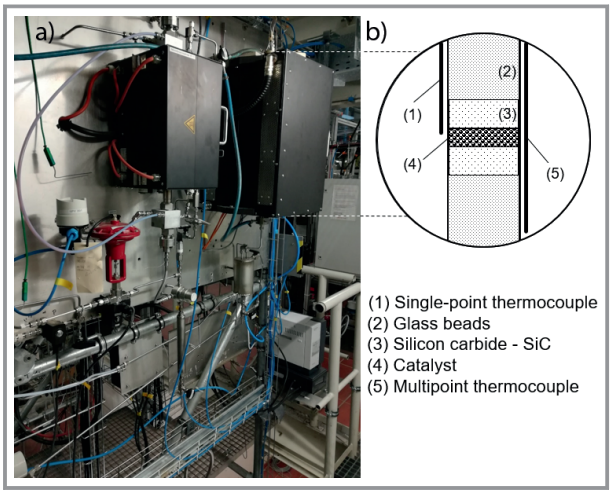

Figure 1. a) Experimental setup at the Technical University of Berlin, b) schematic diagram of the reactor tube.

controllers (MFCs), and the FBR was located inside an electric split tube furnace from HTM Reetz GmbH.

The reactor effluent was cooled, and water was removed. The composition of the outlet gases was analyzed by the Agilent 490 micro-GC. The entire system is controlled and monitored with Simatic PCS 7 by Siemens.

The temperature control was established via a thermocouple placed close to the middle point of the ceramic tube, which served as the furnace setpoint (T_f). Additionally, a second multipoint thermocouple was fixed next to the tube to measure the rector axial temperature profile, the point next to the catalyst bed is considered as the reactor temperature (T_R). The experimental conditions are reported in Tab. 2.

The experiments were performed starting at T_f = 998 K, once the steady state was reached and constant results were recorded, the temperature was increased to the next setpoint at a constant rate (6 K min^{-1}) and in 25 to 50 K steps until T_f reached 1173 K. The reactor is later cooled down using the same rates and steps. The catalyst behavior was constant, and experiments are reproducible.

2.2 Reaction

The OCM reaction experiments were conducted in a dense Al_2O_3 fixed-bed reactor (FBR) with an inner diameter of 7 mm and outer diameter of 10 mm at 1 bar. The tubes were loaded as shown in Fig. 1. Inlet gases were controlled by Bronkhorst mass flow

Table 2. Experimental conditions and dimensions for the setup operation.

CH_4/O_2	N_2 dilution [%]	*GHSV* [h^{-1}]	*T* [K]	Catalyst bed height [mm]	Catalyst weight [g]
4	60	6500	998–1173	20	0.8
4	60	10 000	998–1173	20	0.8
4	60	26 000	998–1173	5	0.2

3 Results and Discussions

3.1 Ignition, Extinction, and Hysteresis (Steady-state Multiplicity)

The O_2 conversion and C_2 yield diagrams for a gas hourly space velocity *GHSV* of 10 000 h^{-1} at standard temperature and pressure (STP) are presented in Fig. 2, showing the ignition-extinction behavior. As soon as the reactor temperature surpasses 1053 K a steep increase in the O_2 conversion is observed, where the catalyst ignition occurs. Afterwards, when increasing the furnace temperature full oxygen conversion is reached at 1103 K.

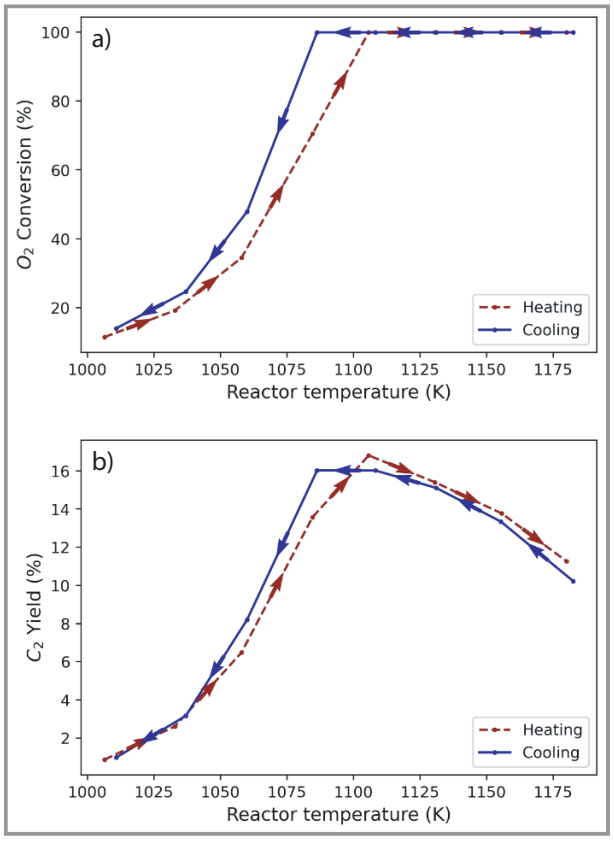

Figure 2. Ignition and extinction behavior of Mn-Na_2WO_4/SiO_2. a) Oxygen conversion and b) C_2 yield at CH_4/O_2 = 4, 60 % N_2 dilution, *GHSV* = 10 000 h^{-1}. The arrows indicate the heating and cooling ramps.

A further increase in temperature leads to a C_2 yield loss due to a drop in selectivity caused by the further oxidation of C_2 hydrocarbons. As the furnace temperature is decreased, the reactor temperature declines slowly and O_2 conversion remains constant until the extinction point is observed as it reaches approximately 1083 K, which is 20 K lower than the operation point during heating. This confirms a state of multiplicity in the reactor.

A considerable drop of C_2 yield is observed when the reactor temperature surpasses 1123 K. This may be attributed to the hot-spot formation caused by the further oxidation of CH_4 and C_2 hydrocarbons to CO and CO_2. Consequently, there is also a decrease on C_2 selectivity with increasing temperature.

A hysteresis effect was detected during the cooling ramp. The yield of C_2 hydrocarbons reaches a plateau in the temperature range of 1083 to 1113 K. This is consistent with the results of Lee et al., who observed a similar behavior at a different reactor diameter (5.08 cm) and using catalyst pellets [14].

3.2 Impact of Contact Time

Previous studies have stated the importance of contact time in the oxidative coupling of methane [15]. In this work, the contact time has been reported in terms of *GHSV*, which can be adjusted by varying the volumetric gas flow or the height of the catalytic bed. As previously indicated in Tab. 2, three different *GHSV* values were evaluated: 6500, 10 000, and 26 000 h^{-1}.

The oxygen and methane conversion versus temperature during the heating and the cooling ramp of the reactor are presented in Fig. 3; each subfigure indicates results at different *GHSV* and constant methane to oxygen ratio. Fig. 3 shows that full O_2 conversion is reached at a different temperature for each *GHSV* value. At lower *GHSV* the ignition point is reached at lower temperatures, there are about 50 K difference between the detection of full oxygen conversion at 26 000 h^{-1} and the other two *GHSV* values.

A longer contact time is also more favorable for the bifurcation regime as a result of thermal backmixing effects.

Fig. 4 demonstrates that multiple steady states are achievable at 26 000 h^{-1}, however, catalyst performance decreases rapidly, which hampers the autothermal reactor operation. Furthermore, C_2 selectivity and yield at shorter contact times are not relevant for a scale-up application in comparison to longer contact times. This means that the ignition-extinction behavior is achievable for thin catalytic beds under certain conditions, where the *GHSV* plays a major role.

4 Conclusion

There are some technical challenges concerning the reactor temperature control that must be overcome for OCM to be implemented industrially. More information and data about the ignition-extinction (hysteresis) behavior of moderately exothermic reactions that can occur in the reactor is essential for a concept development. The results of this work showed some advantages of the thermal effects typical of the OCM reaction entailing an autothermal operation mode, which are associated with a decrease in the hot-spot formation.

Results prove that the Mn-Na_2WO_4/SiO_2 can support autothermal reactor operation, although the operation win-

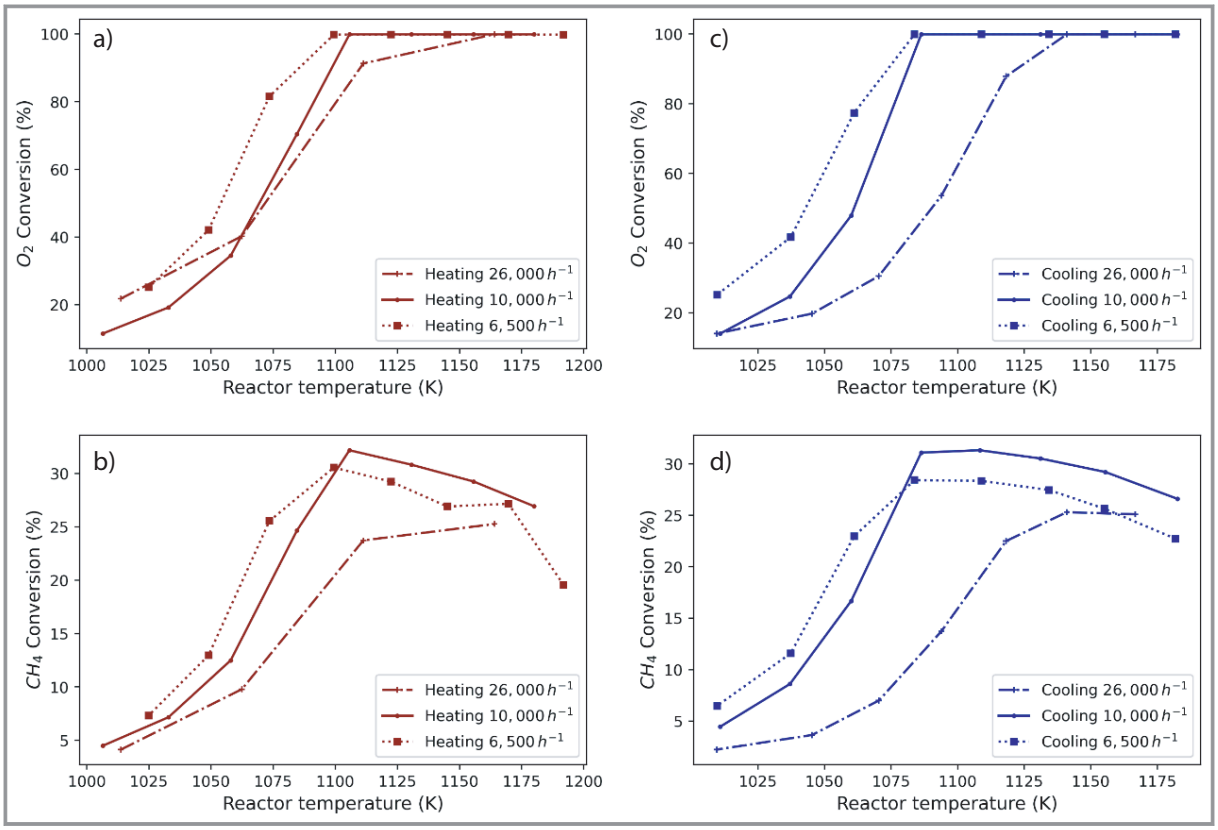

Figure 3. a) Oxygen conversion, and b) methane conversion at different *GHSV* values as the temperature is increased (heating); c) oxygen conversion, and d) methane conversion at different *GHSV* values as the temperature is decreased (cooling) at $CH_4/O_2 = 4$, 60 % N_2 dilution.

dow might not be very broad to allow for a major reduction of the reactor temperature due to the low activity that the catalyst presents at temperatures below 1073 K. However, further investigations should be encouraged to develop a heat recovery concept for this operation mode.

Future studies on the reactor startup conditions, stability tests during longer periods, and optimization of operating conditions need to be performed, as well as a closer look to the potential loss of the catalyst surface area.

This work is supported by the German Federal Ministry of Education and Research (BMBF) funding program Bioeconomy International under grant agreement no. 031B0608A. Open access funding enabled and organized by Projekt DEAL.

Symbols used

GHSV	[h^{-1}]	Gas hourly space velocity
ΔH^0_{Rx}	[kJ mol_{CH4}]	Reaction enthalpy
S	[%]	Selectivity
T	[K]	Temperature
X	[%]	Conversion
Y	[%]	Yield

Sub- and Superscripts

f	Furnace
R	Reactor

Abbreviations

FBR	Fixed bed reactor
MFC	Mass flow controller
OCM	Oxidative coupling of methane

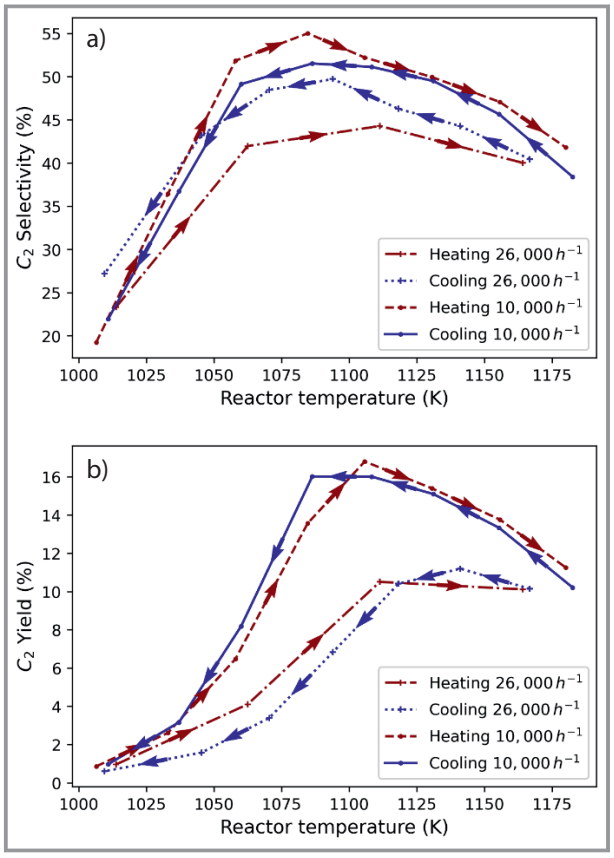

Figure 4. a) C_2 selectivity and b) C_2 yield, for 10 000 h^{-1} and 26 000 h^{-1} at CH_4/O_2 = 4, 60 % N_2 dilution. The arrows indicate the heating and cooling ramps.

References

[1] A. Penteado, E. Esche, D. Salerno, H. R. Godini, G. Wozny, *Ind. Eng. Chem. Res.* **2016**, *55 (27)*, 7473–7483. DOI: https://doi.org/10.1021/acs.iecr.5b04910
[2] B. Beck, V. Fleischer, S. Arndt, M. G. Hevia, A. Urakawa, P. Hugo, R. Schomäcker, *Catal. Today* **2014**, *228*, 212–218. DOI: https://doi.org/10.1016/j.cattod.2013.11.059
[3] Z. Stansch, L. Mleczko, M. Baerns, *Ind. Eng. Chem. Res.* **1997**, *36 (7)*, 2568–2579. DOI: https://doi.org/10.1021/ie960562k
[4] S. Pak, J. H. Lunsford, *Appl. Catal., A* **1998**, *168 (1)*, 131–137. DOI: https://doi.org/10.1016/S0926-860X(97)00340-2
[5] C. Karakaya, H. Zhu, C. Loebick, J. G. Weissman, R. J. Kee, *Catal. Today* **2018**, *312*, 10–22. DOI: https://doi.org/10.1016/j.cattod.2018.02.023
[6] L. Pirro, P. S. F. Mendes, B. D. Vandegehuchte, G. B. Marin, J. W. Thybaut, *React. Chem. Eng.* **2020**, *5 (3)*, 584–596. DOI: https://doi.org/10.1039/C9RE00478E
[7] *Ullmann's Encyclopedia of Industrial Chemistry*, 5th ed., VCH Verlag, Weinheim **1992**.
[8] V. Balakotaiah, Z. Sun, D. H. West, *Chem. Eng. J.* **2019**, *374*, 1403–1419. DOI: https://doi.org/10.1016/j.cej.2019.05.155
[9] S. Arndt, T. Otremba, U. Simon, M. Yildiz, H. Schubert, R. Schomäcker, *Appl. Catal., A* **2012**, *425–426*, 53–61. DOI: https://doi.org/10.1016/j.apcata.2012.02.046
[10] M. R. Lee, M.-J. Park, W. Jeon, J.-W. Choi, Y.-W. Suh, D. J. Suh, *Fuel Process. Technol.* **2012**, *96*, 175–182. DOI: https://doi.org/10.1016/j.fuproc.2011.12.038
[11] J. H. Lunsford, *Angew. Chem., Int. Ed.* **1995**, *34 (9)*, 970–980. DOI: https://doi.org/10.1002/anie.199509701
[12] A. Palmero, J. Hologadovazquez, A. Lee, M. Tikhov, R. Lambert, *J. Catal.* **1998**, *177 (2)*, 259–266. DOI: https://doi.org/10.1006/jcat.1998.2109
[13] J. Wang, L. Chou, B. Zhang, H. Song, J. Zhao, J. Yang, S. Li, *J. Mol. Catal. A: Chem.* **2006**, *245 (1–2)*, 272–277. DOI: https://doi.org/10.1016/j.molcata.2005.09.038
[14] J. Y. Lee, W. Jeon, J.-W. Choi, Y.-W. Suh, J.-M. Ha, D. J. Suh, Y.-K. Park, *Fuel* **2013**, *106*, 851–857. DOI: https://doi.org/10.1016/j.fuel.2013.01.026
[15] N. Yaghobi, *J. King Saud Univ., Eng. Sci.* **2013**, *25 (1)*, 1–10. DOI: https://doi.org/10.1016/j.jksues.2011.06.007